

# Postglacial Uplift

## Physics of the Earth as a Planet, Lecture 7

For a very long time the Scandinavians have known that the land round the northern shores of the Baltic is rising relative to sea level.



Figure 1: Elevated beach terraces on Östergransholm, Eastern Gotland, Sweden.

The enormous extent of the icesheets that formed during the last glaciation became clear in the nineteenth century. All large icesheets are about 3 km thick, and the one that covered northern Europe had a radius of about 1,000 km. Once isostatic compensation was discovered, the explanation of the uplift became clear. When the ice load was emplaced, the mantle flowed to produce compensation. When the ice melted and the load was removed, it flowed back (Figure 2).

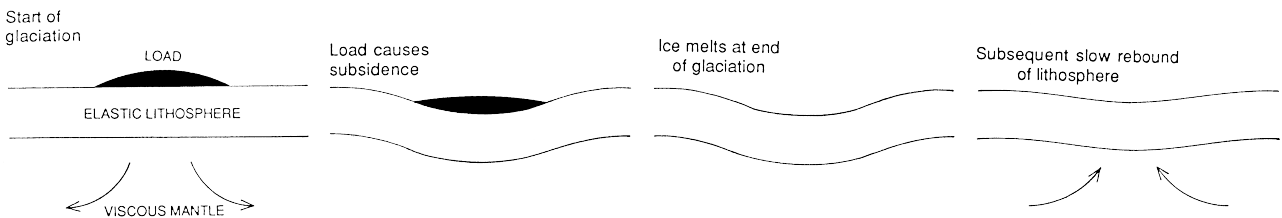


Figure 2: The deformation and uplift which occur as a result of loading and unloading of an elastic lithospheric plate overlying a viscous mantle.

The reason why the land is still rising is that the compensation is incomplete, because the ice only disappeared about 8,000 years ago. A simple model of this behaviour is the flow of a viscous fluid when a depression is formed in its surface. If such a model can be used to describe the uplift and uplift rate, it can provide an estimate of the viscosity  $\eta$  of the mantle. The magnitude of this viscosity is very important, because it controls the convective circulation in the mantle.

To describe the flow we need the equations governing the conservation of mass and momentum in a viscous fluid. Conservation of mass is

$$\frac{\partial \rho}{\partial t} + \nabla \cdot \rho \mathbf{v} = 0, \quad (1)$$

where  $\mathbf{v}$  is the velocity of the fluid, and  $\rho$  its density. We will assume the density of the fluid is constant, in which case (1) simplifies to

$$\nabla \cdot \mathbf{v} = 0, \quad (2)$$

known as the incompressibility relation.

The general expression for conservation of momentum in a fluid is

$$\rho \left( \frac{\partial \mathbf{v}}{\partial t} + \mathbf{v} \cdot \nabla \mathbf{v} \right) = \nabla \cdot \underline{\sigma} - \rho g \hat{\mathbf{z}}, \quad (3)$$

where  $\underline{\sigma}$  is the stress tensor (a symmetric second rank tensor),  $g$  is the acceleration due to gravity, and  $\hat{\mathbf{z}}$  is a unit vector pointing upwards. For an incompressible Newtonian viscous fluid, the relationship between stress and strain rate is given by the constitutive law

$$\sigma_{ij} = -P\delta_{ij} + \eta \left( \frac{\partial v_i}{\partial x_j} + \frac{\partial v_j}{\partial x_i} \right), \quad (4)$$

where  $P$  is the pressure and  $\eta$  is the dynamic viscosity (which we will also assume constant). Substituting (4) into (3), and combining with (2) yields the famous Navier-Stokes equations

$$\rho \left( \frac{\partial \mathbf{v}}{\partial t} + \mathbf{v} \cdot \nabla \mathbf{v} \right) = -\nabla P + \eta \nabla^2 \mathbf{v} - \rho g \hat{\mathbf{z}}. \quad (5)$$

For the mantle, because the viscosity is so large (as we shall soon see), and because the flow speeds are so slow, we can neglect the left hand side of this equation. What remains is the equation governing slow viscous flow, the Stokes equation,

$$0 = -\nabla P + \eta \nabla^2 \mathbf{v} - \rho g \hat{\mathbf{z}}. \quad (6)$$

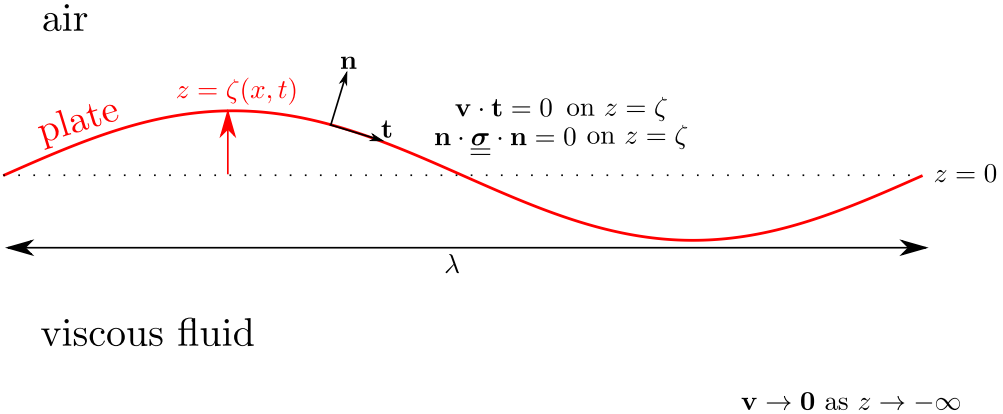


Figure 3: Viscous half space model of postglacial rebound.

We want the solution to (2) and (6) when the flow is driven by a small deformation to the upper surface of a viscous half space (Figure 3). The simplest problem is when the flow is two-dimensional, when it can be described by a stream function  $\psi(x, z)$

$$\mathbf{v} = (u, 0, w) = \nabla \times (0, \psi, 0) = \left( -\frac{\partial \psi}{\partial z}, 0, \frac{\partial \psi}{\partial x} \right). \quad (7)$$

Notice that the stream function formulation ensures that mass conservation (2) is obeyed,

$$\nabla \cdot \mathbf{v} = \frac{\partial u}{\partial x} + \frac{\partial w}{\partial z} = 0. \quad (8)$$

Equation (6) can be simplified by taking its curl

$$\nabla^2 \nabla \times \mathbf{v} = 0. \quad (9)$$

Substituting (7) gives

$$\nabla^4 \psi = 0, \quad (10)$$

the biharmonic equation. We can simplify the equations by splitting into Fourier components in the  $x$  direction

$$\psi = \Psi(z)e^{ikx}, \quad k = \frac{2\pi}{\lambda}, \quad (11)$$

and (10) becomes

$$\left( \frac{d^2}{dz^2} - k^2 \right)^2 \Psi = 0. \quad (12)$$

Substitution of

$$\Psi = A e^{\sigma z}, \quad (13)$$

gives the auxiliary equation

$$(\sigma^2 - k^2)^2 = 0. \quad (14)$$

Clearly  $\sigma = \pm k$  gives two solutions, but (12) is a fourth order equation, and therefore must have four solutions to satisfy the boundary conditions. Because  $\sigma = \pm k$  are repeated roots, the full solution is

$$\Psi = (A + Bz)e^{kz} + (C + Dz)e^{-kz}. \quad (15)$$

The fluid extends below  $z = 0$ , and the velocity must vanish as  $z \rightarrow -\infty$ . Therefore  $C$  and  $D$  must be zero, and

$$\psi = (A + Bz)e^{kz+ikx}. \quad (16)$$

Substituting (16) into (7) gives the velocities as

$$u = -\frac{\partial \psi}{\partial z} = -(B + kA + kBz)e^{kz+ikx}, \quad (17)$$

$$w = \frac{\partial \psi}{\partial x} = ik(A + Bz)e^{kz+ikx}. \quad (18)$$

Note that while the expressions given here for the velocities are complex, it is only the real parts that are physical (i.e. the physical solution is in terms of sines and cosines rather than complex exponentials). Using complex exponentials simply makes the algebraic manipulations a little easier. Substituting these velocity expressions into the momentum equation (6) yields

$$\frac{\partial P}{\partial x} = -2\eta k^2 B e^{kz+ikx}, \quad (19)$$

$$\frac{\partial P}{\partial z} = -\rho g + 2i\eta k^2 B e^{kz+ikx}, \quad (20)$$

from which the pressure can be obtained by integration as

$$P = -\rho g z + \mathcal{P}, \quad (21)$$

$$\mathcal{P} = 2\eta i k B e^{kz+ikx}. \quad (22)$$

The arbitrary constant associated with the integration has been set such that the pressure is zero at the surface when the surface is flat. Note that the pressure has been split into two parts: the hydrostatic part ( $-\rho g z$ ) and the perturbation  $\mathcal{P}$  due to fluid flow.

We now need to apply the boundary conditions at the surface. These boundary conditions are complicated by the fact that the surface is deformed, but to simplify the analysis we will assume that the amplitude of this surface deformation is small. The surface is at  $z = \zeta$  where

$$\zeta = \varepsilon e^{ikx} \quad (23)$$

and we will assume that  $k\varepsilon \equiv 2\pi\varepsilon/\lambda \ll 1$  (a long wavelength approximation). For the post-glacial problem this is clearly a good approximation, because the compensated depression of the surface is only about 1 km when loaded with 3 km of ice, and the wavelength is about 3,000 km.

On the surface  $z = \zeta$  we will assume that the tangential component of the velocity  $\mathbf{v} \cdot \mathbf{t}$  vanishes, because there is a plate on top, and that the normal stress  $\mathbf{n} \cdot \underline{\underline{\sigma}} \cdot \mathbf{n}$  also vanishes (the air exerts no normal stress). With a small deformation of the interface the boundary conditions can be linearised: we will perform a Taylor series expansion of the boundary conditions in the small parameter  $\varepsilon$  and neglect terms of order  $\varepsilon^2$  or higher. It is important to note that the velocities  $u, w$  and the perturbed pressure  $\mathcal{P}$  are all  $\mathcal{O}(\varepsilon)$  because they vanish when the interface is flat (no fluid flow). It follows that the unknown constants  $A$  and  $B$  we want to find are  $\mathcal{O}(\varepsilon)$ . The boundary condition

$$\mathbf{v} \cdot \mathbf{t} = 0 \text{ on } z = \zeta. \quad (24)$$

is straightforward to linearise. To leading order we can approximate the tangential vector by a unit vector in the horizontal,  $\mathbf{t} \approx \hat{\mathbf{x}}$ , so  $\mathbf{v} \cdot \mathbf{t} \approx u$ , the horizontal component of the velocity. Consider the Taylor series expansion of the horizontal velocity  $u(x, z)$  at the surface  $z = \zeta$ ,

$$u(x, \zeta) = u(x, 0) + \zeta \frac{\partial u}{\partial z}(x, 0) + \dots \quad (25)$$

Since both  $u$  and  $\partial u / \partial z$  are  $\mathcal{O}(\varepsilon)$ , and  $\zeta$  is  $\mathcal{O}(\varepsilon)$ , we can approximate  $u(x, \zeta) \approx u(x, 0)$  at leading order in  $\varepsilon$ . Thus the boundary condition on the velocity at first order is simply that the horizontal velocity vanishes on the undeformed surface, namely

$$u = 0 \text{ on } z = 0, \quad (26)$$

and hence from (17)

$$B + kA = 0. \quad (27)$$

The first order boundary condition on the normal stress is more subtle. It is *not*  $\sigma_{zz} = 0$  on  $z = 0$ . The boundary condition to linearise is

$$\mathbf{n} \cdot \underline{\underline{\sigma}} \cdot \mathbf{n} = 0 \text{ on } z = \zeta. \quad (28)$$

It is helpful to split the stress tensor into a hydrostatic part, and a part due to the flow:  $\underline{\underline{\sigma}} = \rho g z \underline{\underline{I}} + \widetilde{\underline{\underline{\sigma}}}$ , where  $\underline{\underline{I}}$  represents the identity tensor. It follows that

$$\mathbf{n} \cdot \widetilde{\underline{\underline{\sigma}}} \cdot \mathbf{n} \Big|_{z=\zeta} = -\rho g \zeta. \quad (29)$$

Similar to the argument in (25), since  $\widetilde{\underline{\underline{\sigma}}}$  is  $\mathcal{O}(\varepsilon)$  the term on the left can be expanded to leading order using  $\mathbf{n} \approx \hat{\mathbf{z}}$  as

$$\widetilde{\sigma}_{zz} \Big|_{z=0} = -\rho g \zeta. \quad (30)$$

Using the constitutive law for the stress tensor, the above becomes

$$\left( -\mathcal{P} + 2\eta \frac{\partial w}{\partial z} \right) \Big|_{z=0} = -\rho g \zeta. \quad (31)$$

In fact, the term due to  $\partial w/\partial z$  in the above is zero. This can be seen as follows:  $u = 0$  on  $z = 0$  from (26)  $\Rightarrow \partial u/\partial x = 0$  on  $z = 0 \Rightarrow \partial w/\partial z = 0$  on  $z = 0$  from (8). It then follows that

$$\mathcal{P} = \rho g \zeta \text{ on } z = 0, \quad (32)$$

and hence from (22)

$$2\eta ikB = \rho g \varepsilon. \quad (33)$$

Combining (27) and (33) we have

$$A = \frac{i\rho g \varepsilon}{2\eta k^2}, \quad B = -\frac{i\rho g \varepsilon}{2\eta k}. \quad (34)$$

Therefore the velocities (17) and (18) are given in terms of the surface deformation as

$$u = \frac{i\rho g \varepsilon}{2\eta} z e^{kz+ikx}, \quad (35)$$

$$w = -\frac{\rho g \varepsilon}{2\eta k} (1 - kz) e^{kz+ikx}. \quad (36)$$

Though the above expressions are in fact the solution to the problem, they do not at first appear to be any use. We want to calculate the shape of the surface as a function of time, and what we have ended up with is an expression for the velocities in terms of the surface deformation. There is in fact one more boundary condition we need to apply, known as the kinematic boundary condition, that specifies how the surface evolves through time. To first order, this kinematic boundary condition is given by

$$\frac{\partial \zeta}{\partial t} = w \text{ on } z = 0, \quad (37)$$

namely that the rate at which the surface  $\zeta$  uplifts is equal to the vertical velocity  $w$ . Hence from (23) and (36) we have

$$\frac{d\varepsilon}{dt} = -\frac{\rho g}{2\eta k} \varepsilon, \quad (38)$$

which is the standard equation for exponential decay with a time constant  $\tau$

$$\tau = \frac{2\eta k}{\rho g} \equiv \frac{4\pi\eta}{\rho g \lambda}. \quad (39)$$

This equation shows that the time constant increases with increasing  $\eta$ , and decreases with increasing  $\rho$  and  $g$ , all of which is sensible. What is perhaps less obvious is that it should *decrease* as  $\lambda$  increases. We can easily show that this equation is correct by dimensional arguments. We wish to construct a quantity with the dimensions of time from  $\eta$ ,  $\rho$ ,  $g$  and  $\lambda$ . Since

$$\left[ \frac{\eta}{\rho} \right] = \frac{L^2}{T}, \quad [g] = \frac{L}{T^2}, \quad [\lambda] = L, \quad (40)$$

the combination

$$\frac{\eta}{\rho g \lambda} \quad (41)$$

has the dimensions of time. But we need to solve the problem properly to get the factor  $4\pi$ . If we did not, and simply used (41), our estimate of  $\eta$  would be wrong by an order of magnitude.

There are a number of ways to use (38) and (39) to estimate  $\eta$ . If  $\tau$  can be estimated directly, then  $\rho$  ( $= 3.3 \text{ Mg m}^{-3}$ ) and  $g$  ( $= 9.8 \text{ m s}^{-2}$ ) are known and  $\lambda$  can be estimated from the shape of the ice load. Figure 5 shows the uplift history of the Angerman river in Sweden, from which

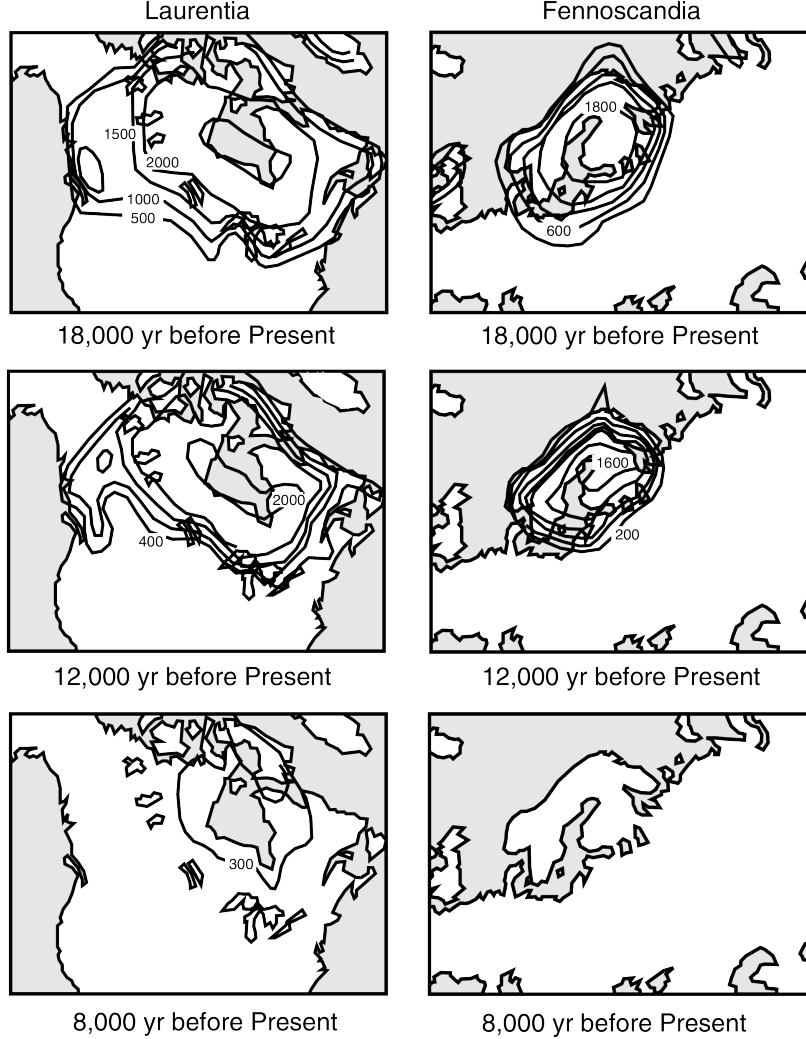


Figure 4: Deglaciation chronology for Laurentia (left) and Fennoscandia (right). Contours show the estimated ice sheet thickness in m.

a time constant  $\tau = 4,400$  years can be inferred. The wavelength  $\lambda$  of the Fennoscandian ice sheet is about 3,000 km, so

$$\eta = \frac{\rho g \lambda \tau}{4\pi} \simeq 1 \times 10^{21} \text{ Pa s.} \quad (42)$$

An alternative method of estimating the time constant is by looking at the gravity anomaly. The present day gravity anomaly can be approximated by

$$\Delta g = 2\pi G \rho \zeta. \quad (43)$$

The initial gravity anomaly  $\Delta g_0$  is

$$\Delta g_0 = 2\pi G \rho_w t, \quad (44)$$

where  $\rho_w$  is the ice density ( $= 1.0 \text{ Mg m}^{-3}$ ) and  $t$  is the ice thickness ( $\simeq 3 \text{ km}$ ). Therefore  $\Delta g_0 \sim 120 \text{ mGal}$  (recall that  $2\pi G \approx 42 \text{ mGal m}^3 \text{ Mg}^{-1} \text{ km}^{-1}$ , so  $\Delta g_0 = 42 \times 1.0 \times 3 \text{ mGal}$ ). Since the time when the ice melted,  $\tau_0$ , is known,  $\tau$  can be estimated from

$$\frac{\tau_0}{\tau} = -\ln \left( \frac{\Delta g}{\Delta g_0} \right). \quad (45)$$

Since the ice disappeared more than 8,000 years ago (Figure 4), the gravity anomaly should have decayed to about 16% of its initial value, and should be about 20 mGals, which agrees with the gravity anomaly map (Figure 9).

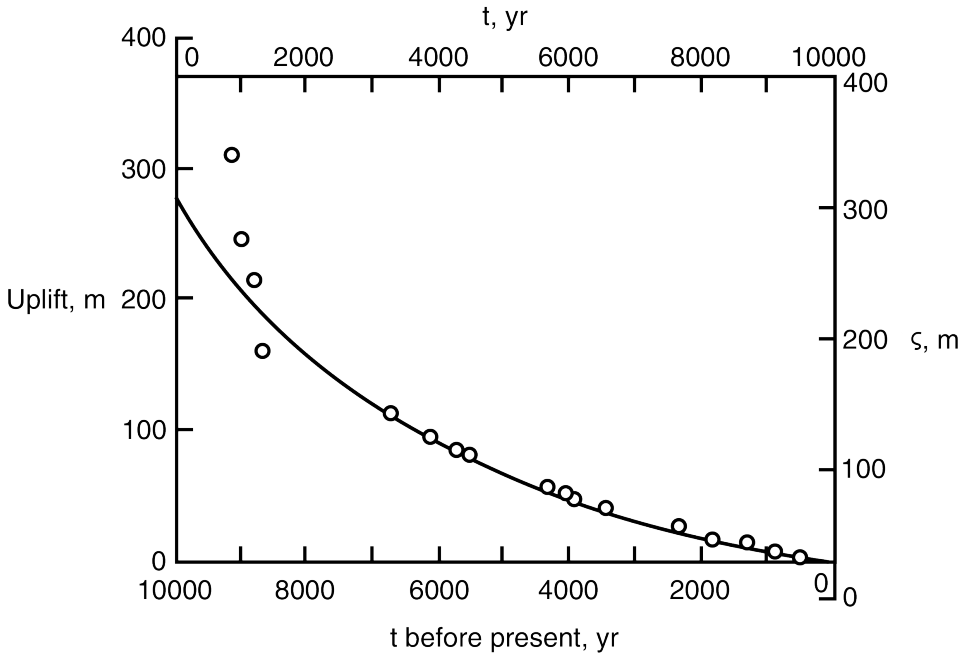


Figure 5: Elevation of dated fossil beach terraces at the mouth of the Angerman river in Sweden (circles). Solid line shows a model fit to these data. The model fit has a time constant  $\tau = 4,400$  years.

It is now possible to observe present day postglacial uplift with satellites. Figure 7 shows the uplift as estimated by continuously recording GPS, and is in good agreement with the earlier geological estimates of present day peak uplift on the order of  $9 \text{ mm yr}^{-1}$  (Figure 6). It is also possible to see the changes in the free air gravity anomaly over time. We can estimate what this should be from

$$\frac{\partial \Delta g}{\partial t} = 2\pi G \rho \frac{\partial \zeta}{\partial t}. \quad (46)$$

With an uplift rate of  $\partial \zeta / \partial t \sim 9 \text{ mm yr}^{-1}$  the change in the gravity anomaly  $\partial \Delta g / \partial t \sim 1.2 \mu\text{Gal yr}^{-1}$  which is indeed what is observed (Figure 8).

The ice sheet in Canada disappeared at much the same time as the one in Northern Europe (Figure 4), but the gravity anomaly is still about 50 mGal (Figure 10) and there is some evidence from the uplift that the time constant is larger. This difference is unexpected. Because the icesheet was larger ( $\lambda \sim 8,000 \text{ km}$ ) than the one in northern Europe, the time constant would be expected to be shorter, not longer. The uplift gives a time constant of  $\sim 6,600$  years, giving

$$\eta \sim 4 \times 10^{21} \text{ Pa s}, \quad (47)$$

and the gravity anomaly suggests  $\tau \sim 8,000$  years if the ice melted 7,000 years ago. The most likely explanation of this difference is that the mantle viscosity increases with depth, and that the flow produced by the Canadian icesheet ‘feels’ the viscosity at greater depth than does that of Fennoscandia.

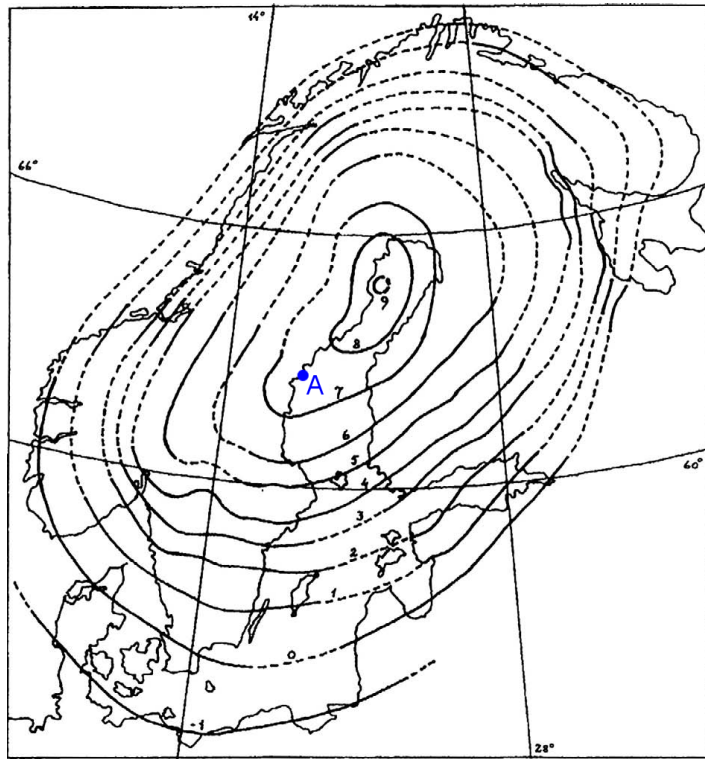


Figure 6: Present day uplift rate of Fennoscandia determined by geological observations. Contours are in  $\text{mm yr}^{-1}$ . The maximum uplift is around  $9 \text{ mm yr}^{-1}$ . The mouth of the Angerman river is marked as ‘A’ (see Figure 5).

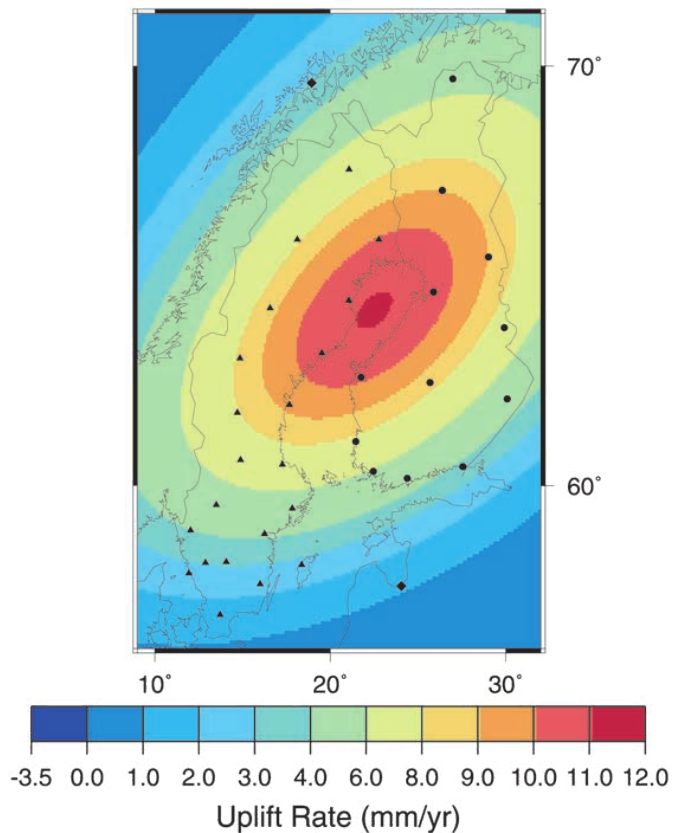


Figure 7: Present day uplift rate of Fennoscandia determined by continuous GPS monitoring. GPS stations are show as dots and triangles. Contours show a Gaussian fit to the GPS data.

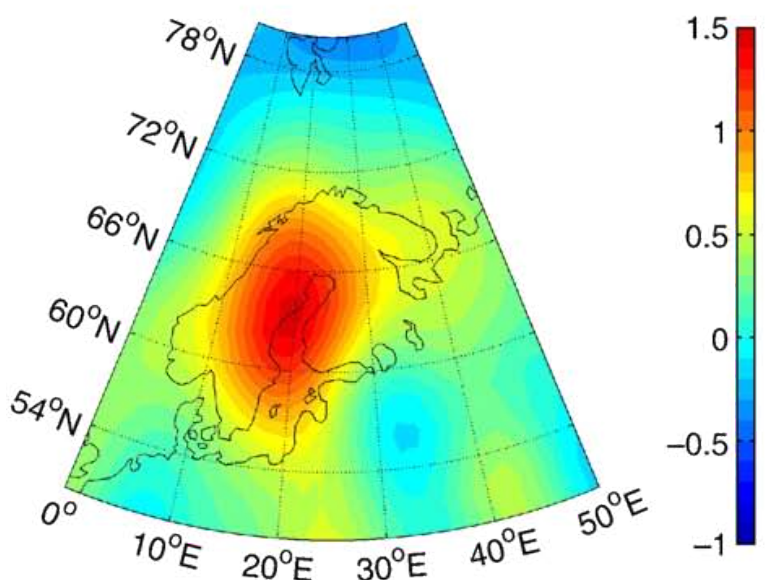


Figure 8: Secular gravity variation in Fennoscandia determined from GRACE monthly solutions. Units are  $\mu\text{Gal yr}^{-1}$ .

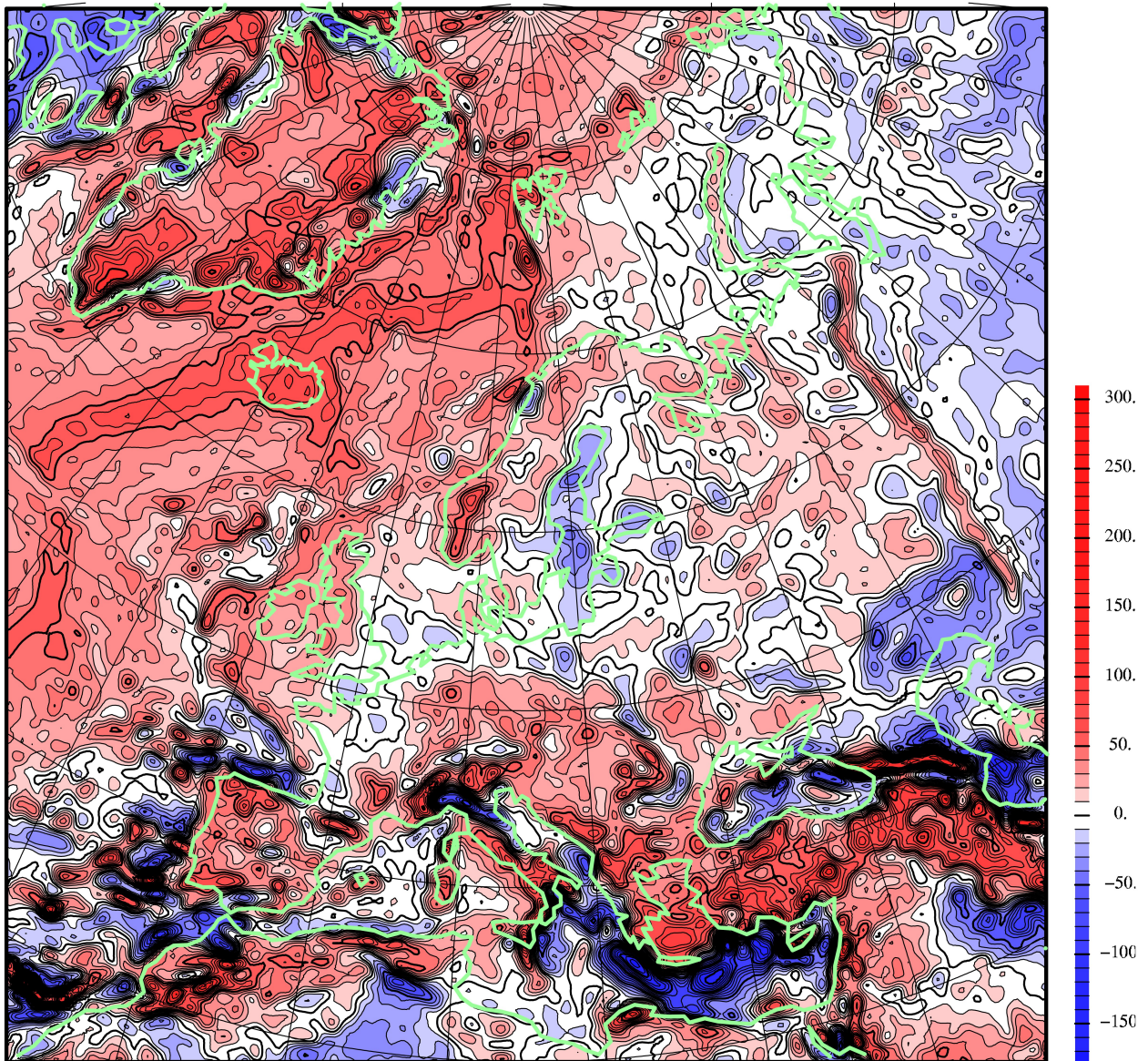


Figure 9: Long wavelength free air gravity anomaly map of Europe. Scale is in mGals.

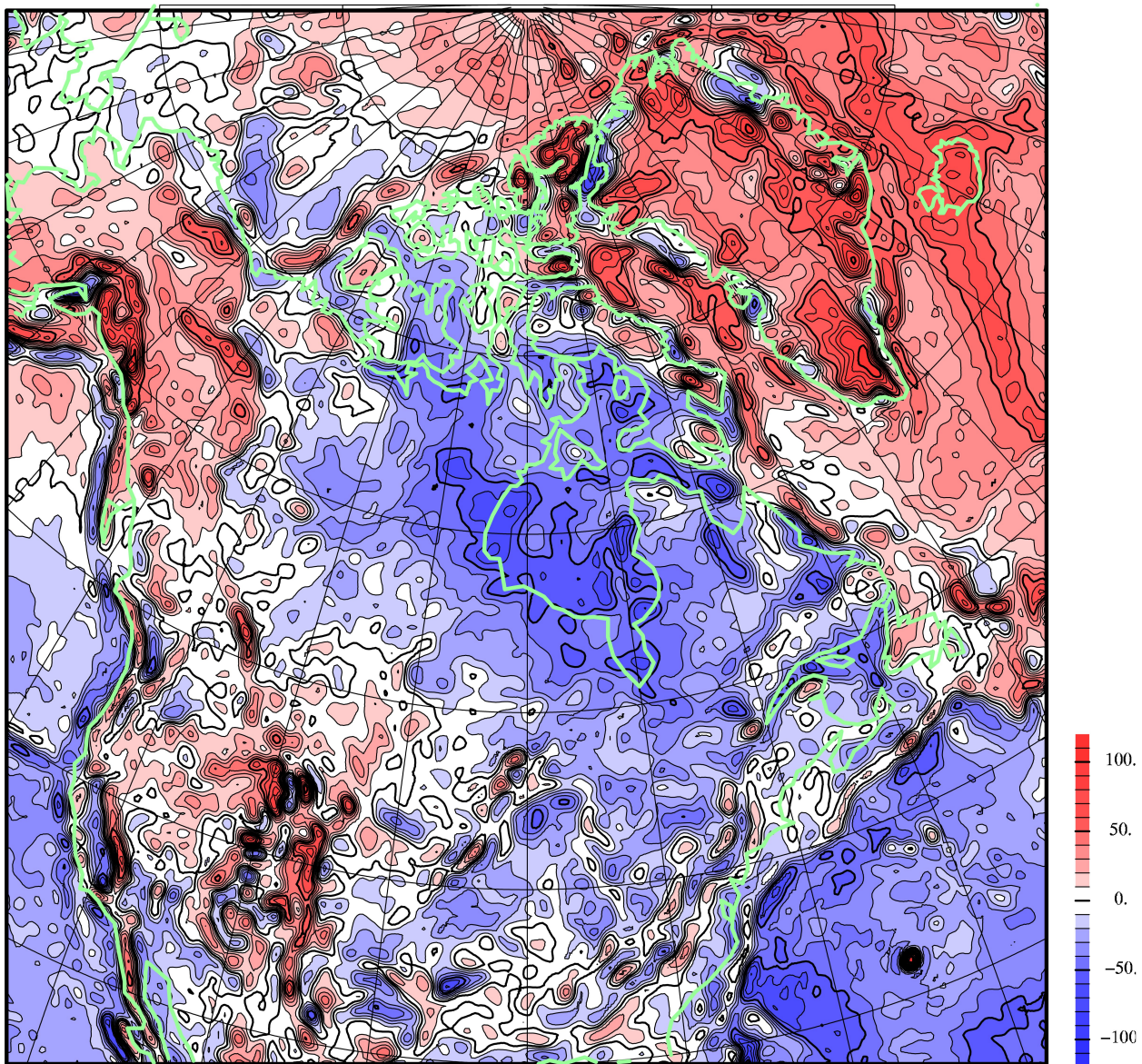


Figure 10: Long wavelength free air gravity anomaly map of North America. Scale is in mGals.